

THEORETICAL DESIGN AND MOTION MODELING OF AN ELECTROMAGNETIC MECHANICAL SPEED BUMP HARVESTER

Hatem Hadi Obeid¹, Abdul Kareem Jaleel², and Nazar Aubays Hassan³

Department of Mechanical Engineering, Babylon University at Babylon City of Iraq

(E-mails: drhatemhadi@yahoo.com, drkareem959@yahoo.com, nzaied@yahoo.com)

ABSTRACT :-

This paper suggests a new mechanical design able to harvest dynamic wasted vehicles impact energy by Road- Bumps. Mechanical Speed Bump design is difference the traditional, where it's including many moving parts such as camshaft system, epicyclic gear train system, one way clutch system, flywheel system and generator system. Camshaft system is used to convert liner transient motion into rotational, while epicyclic gear train system is used to convert and control motion. Flywheel system is used to storage an extra energy and generator system is used to convert kinetic energy into electricity. The kinematics and dynamics of motion mechanism and generator are considered. Dynamic model has been derived and analyzed for epicyclic gear train and permanent magnets generator, based on differential equations. Governing differential equations are solved numerically by expression of Duhamel Integral. Results and simulations are carried out to study design features. Design harvested powers are estimated. Guidelines are given to improve this type of energy harvester in future.

Key words: mechanical speed pump, camshaft system, one way clutch system, gear train system, friction damping coefficient and electrical damping coefficient.

الخلاصة :-

يقترح البحث الحاضر تصميمًا ميكانيكيًا جديدًا لمطبة الطريق بحيث تكون قادرة على حصد الطاقة الديناميكية الضائعة جراء تصادم إطارات المركبات مع مطبة الطريق عند عبورها. يختلف التصميم المقترح لمطبة الطريق الميكانيكية عن المطبة الاعتيادية كونها تحتوي على أجزاء متحركة كثيرة مثل: منظومة عمود الحدبات ومنظومة التروس الكواكبية و منظومة الفاصل الميكانيكي للحركة ومنظومة الدوالب الطيار إضافة إلى منظومة المولد الكهربائي. تعمل منظومة عمود الحدبات على تحويل الحركة الخطية إلى دورانية بينما تعمل المنظومة الكواكبية على رفع نسبة التحويل والسيطرة عليها أما منظومة

الدولاب الطيار فإنها تعمل على تخزين الطاقة الفائضة بينما تعمل منظومة المولد الكهربائي على تحويل الطاقة الحركية إلى طاقة كهربائية. جميع الكتل المتحركة المؤثرة داخل التصميم المقترح قد تم اعتبارها وتحليل حركتها تحليلًا تفصيليًا ولكلا جزئي التصميم الميكانيكي والمولد الكهربائي. المعادلات الحركية تم اشتقاقها و نمذجتها على شكل معادلات تفاضلية ولكلا المنظومتين المنظومة الكواكبية ومنظومة المولد الكهربائي ذات الفيض المغناطيسي الدائم. المعادلات الحاكمة تم تعريفها على صيغة تكامل "دوهامل" ومن ثم حلها بالطرق العددية. تم عمل محاكات للنموذج المقترح وحصد النتائج ليسنى لنا دراسة خصائص التصميم إضافة إلى ذلك فإنه قد تم تخمين كمية الطاقة المكتسبة من التصميم ووضع التوصايا والإرشادات الأزمنة لتحسين أداء التصميم مستقبلاً.

كلمات رئيسية : مطبة الطريق الميكانيكية، منظومة عمود الحدبات، منظومة الفصل الميكانيكية، المنظومة الكواكبية، معامل التخميد الاحتكاكي ومعامل التخميد الكهربائي .

Symbol	Meaning	Units
F_a, F_c, F_{ca}, F_s and F_g	Friction Damping Coefficient of each of Annular Gear, Planetary Carrier, camshaft, Planetary Gear and Sun Gear respectively.	N.m.s/rad
Dem	Electromagnetic Damping Torque Coefficient of Generator	N.m.s/rad
$I_a, I_c, I_{ca}, I_g, I_f, I_{G1},$ I_{G2} and I_s	Inertia of each of Annular Gear, Planetary Carrier, Camshaft System, Planetary Gear, Flywheel, Gear No.1, Gear No. 2 and Sun Gear respectively.	kg.m ²
$j\omega l$	Coil Imaginary Impedance	Ohm
k_1, k_2	Camshaft Return Spring and Twisting Spring Respectively.	N.m/rad
P_o	Output Power	Watt
N_{c1}, N_{e1}	Planetary Carrier and Planetary Gear Motion Ratio Relative to Sun Motion	Without
N_{c2}, N_{e2}	Planetary Carrier and Planetary Gear Motion Ratio Relative to Annular Motion	Without
$r_a, r_g, r_{G1},$ r_{G2} and r_s	Radius of Annular, Planetary, Gear No.1, Gear No. 2 and Sun Gear respectively.	M
R	Electrical Coil Resistance	Ohm
T	Impact Load Time Interval	Sec
T_r	Torque Required to Drive the Electromagnetic Generator	N.m/rad
$T_u(t), T_{u1}, T_{u2}$	Input Torque and Its Two Components in Time Domain	N.m
T_{p1}, T_{p2}	Input Torque Components in Principal Domain	N.m
V_v	Vehicle speed	m/sec
X	Horizontal Distance That Vehicle Needs To Complete Stroke.	M
θ and θ_f	Angular Displacement of Generator Core and Flywheel, respectively.	Rad

Φ	Magnetic Flux Leakage Throw The Coils	Webber
Ωf	Angular Speed of Flywheel system.	rad/sec
β_1, β_2	Motion of System Coordinates that's Defined as Sun and Annular motions in Time Domain	Rad
$\beta_{p1}, \beta_{p2}, \dot{\beta}_{p1}, \dot{\beta}_{p2}$ $\ddot{\beta}_{p1}, \ddot{\beta}_{p2}$	Motion, Velocity and Acceleration of System of Two Components Coordinates in Principal Domain	Rad, rad/sec, rad/s ²
ω_1, ω_2	System Natural Frequencies	rad/sec
Others	Are Define According to Location	---

1- INTRODUCTION :-

Automobiles are utilized all around the world and provide their users with a highly convenient means of transportation. Despite their benefits, automobiles, in general, are a significant contributor to the energy and environment issues that we are facing today, yet only 10-16% of that fuel energy is used to actually drive the vehicle (to overcome the resistance from road friction and air drag (Zhang 2009). Vehicles dissipate (waste) a large portion of their energy in the form of kinetic energy through their braking and suspension systems However, research and development of mechanism able to convert vehicle wasted energy into useful power remains in the primary stage (Karnopp 1989). Several researchers have explored the concept of regenerative vehicle suspension to harvest power from mass-spring vibration energy, like Zuo et al that is designed a linear electromagnetic energy harvester capable of generating more than 16-64 watts of energy from all four shock absorbers with 0.25-0.50 m/s RMS suspension velocity. (Suda 1998)

A large number of vibration-based on Energy Harvesting Devices (EHDs) have been proposed to harvest power using various mechanisms, including electromagnetic, electrostatic, and piezoelectric (Goldner 2001 and Ebrahimi 2001). Among them, piezoelectric EHDs have received more attention due to their self-contained power generation capability, but higher power quantities are just promised for the near future by means of optimized design and improved materials. A new design of speed bump for recovering energy from traveling vehicles and some investigations have been conducted to apply this kind of devices. Very few attempts in this field exist in literature, for example with piezoelectric (Zuo 2010) and hydraulic systems (Martins 2009), but here the authors focused on a completely different device.

Power bumps are innovative energy harvesting devices similar to mechanical speed humps but recover the energy wasted by vehicle brakes in decelerating lanes. They reduce speed, produce electric energy (Avadhany 2009) and increase road safety at the same time.

The main scope of this paper is studying harvesting ability of the vehicle's impacts energy by suggestion a special mechanical speed bump and estimation amount of harvesting power at speed range (20-50km/hr) to investigate building of "Recharging Station of Electrical vehicles" depending on the harvesting energy without more oil burning needs in future applications.

2. DESCRIPTION OF THE SUGGESTION DESIGN :-

Mechanical Speed Bump (MSB) design is a special gearing system install as separated cells in the mid-road against to vehicles motion. A group of power cells are connecting together and assembled in parallel to increase impact probability. Any cell of MSB includes many mechanical parts, as, camshaft system, spur gears system, epicyclic gear train system, separated clutch system, and electromagnetic generator system. Camshaft system is design to receive vehicles impacts energy. Ramp dimensions of (MSB) are similar to the dimensions of the traditional speed bump body, excepted it has 0.12m extend base in depth underground. Cells appearing dimensions are 0.6m length, 0.5m width and 8cm height, as shown in **Fig.1**.

In the suggestion design any power cell has four steel cams assembled with steel shaft by welding. Gear No.1 has coupled directly with one camshaft terminals without slipping. Gear No.2 has meshed with Gear No.1 and used to transmit energy into input shaft of Epicyclic Gear Train System (EGTS) over mechanical one direction clutch. Clutch is used to separate the camshaft from main system and allow it to return back when vehicle impact end. In general, simple EGTS has three main motions; planetary gear carrier, sun gear, and annular gear motions. To make up an output /input motion ratio one of three motions should have fixed. While, the suggestion design is modified to have three motions in the same time, where fixed gear theory is instead of movable twisting gear-spring system. The new modification makes output/input motion ratio of EGTS able to vary automatically depending on many conditions such as impact time interval, amount of twisting stiffness and condition of system response. Flywheel-generator system is designed to be driven by EGTS over second mechanical clutch to separate and harvest flywheel kinetic energy after impact stroke end, as shown in **Fig. 2**.

3. SYSTEM MODELING :-

Modeling of MSB system will be divided it into three regions, as shown in **Fig. 3**. And governing equating will be derived as a two degree of freedom mechanical system with an electromagnetic damping system. Governing differential equations will be expression in Duhamel Integral and solved numerically.

3.1. Input Torque (Input Region)

A constant weight and dimensions of vehicle's wheels (tires) have assumed to make smulation, as (diameter=0.7m and 250kg). Motion of the camshaft with time is controlled by the outside shape surface of the cams itself and vehicle speed. Cam-tire tangential point varying with vehicle forward motion, therefore input torque will be varying with time. Camshaft angle will be changing with time from (45°) to the zero. 3D max program simulation has carried out to calculate time history of input torque by calculating all symbols that are showing in **Fig. 4**.

Let (T) is a total load time interval and it's can be defines as:

$$T = X/V_v \quad (1)$$

For proposed tire diameter =0.7 m, Then by 3d max program simulation: X=0.24m and time step is

$$dt = T/8.$$

Then, we can calculate of each of following samples as a camshaft angle variation (θ), cam active torque distance (d), and amount of active input torque (T_u), as shown in **Table 1** and according to symbols definitions in **Fig. 4** and result of 3Dmax program design simulation.

3.2. Epicyclic Gear Train System (Control Region)

Any simple epicyclic gear train system should have many moving parts as a sun gear, annular gear, planetary gear, and planetary carrier. Relative velocity of any inside gear depends on its diameter and type of motion, as shown in **Fig. 5**. In the suggestion design planetary carrier is regarded as the epicyclic input motion and coupled directly with gear No.2, sun gear is involved to drive flywheel- generator system as the output, annular gear is involved to twist the control spring and regarded as the semi-fixed gear. Motions of the system coordinates (β_1, β_2) are defined according to the sun gear motion and annular gear motion, respectively. Then, **angular** displacement and velocity of planetary carrier and planetary gear will be derived relative to the system coordinates (β_1, β_2), as the following (Marians 1987)

$$\theta_c = \left[\frac{r_s}{2(r_s + r_a)} \right] \beta_1 + \left[\frac{r_a}{2(r_s + r_a)} \right] \beta_2$$

or

$$\theta_c = [N_{c1}] \beta_1 + [N_{c2}] \beta_2 \quad (2)$$

And

$$\theta_s = \left[\frac{r_s}{2} \left(\frac{1}{(r_s + r_a)} - \frac{1}{r_s} \right) \right] \beta_1 + \left[\frac{r_a}{2} \left(\frac{1}{(r_s + r_a)} + \frac{1}{r_s} \right) \right] \beta_2$$

Or

$$\theta_s = [N_{s1}] \beta_1 + [N_{s2}] \beta_2 \quad (3)$$

3.3. Flywheel-Generator System (Output Region)

In general, any electromagnetic generator (EMG) consists of wound copper coils, and magnetic field source. Voltage develops in the coil's circuit proportionally with developing of the magnetic field source relative velocity. Current flow in the close load circuit (coil turns) produce in side magnetic field opposite in direction with original magnetic field, thus, rotating shaft will be resist. Amount of magnetic opposite torque depends on the value of current flow in load circuit. The resistance torque effect as a damping system. Opposite torque is effect directly on the flywheel rotating time. However, properties of the EMG circuit limit the amount of the system damping coefficient. **Fig. 6** shows the essential EMG elements, and resistant circuit diagrams. In order to extract power from the generator, the coil terminals must be connected to a load resistance (R_L) allowing a current to flow in the coil. The interaction between the field caused by the induced current and the field from the magnets gives rise to a torque which opposes the rotation and is proportional to the current and velocity of generator core.

$$T_r = D_{em} \frac{d\theta}{dt} \quad (4)$$

Maximizing of the electromagnetic damping D_{em} and angular speed of the generator core is leading to maximization of required torque. Electromagnetic generator damping D_{em} depends

on amount of flux linkage gradient and coil impedance (Priya 2009) and can be defined as the following:

$$D_{em} = \frac{1}{R_L + R + j\omega L} \left(\frac{d\Phi}{d\theta} \right)^2 \tag{5}$$

The idea will be maximize the flux linkage gradient and minimizing the coil Impedance to improve output power. Then, generator instant output power can be defined as:

$$P_o = T_r(t) \frac{d\theta}{dt} \tag{6}$$

Sub equation (4) in (6) to get electromagnetic output power (Priya 2009):

$$P_o = D_{em} \left(\frac{d\theta}{dt} \right)^2 \tag{7}$$

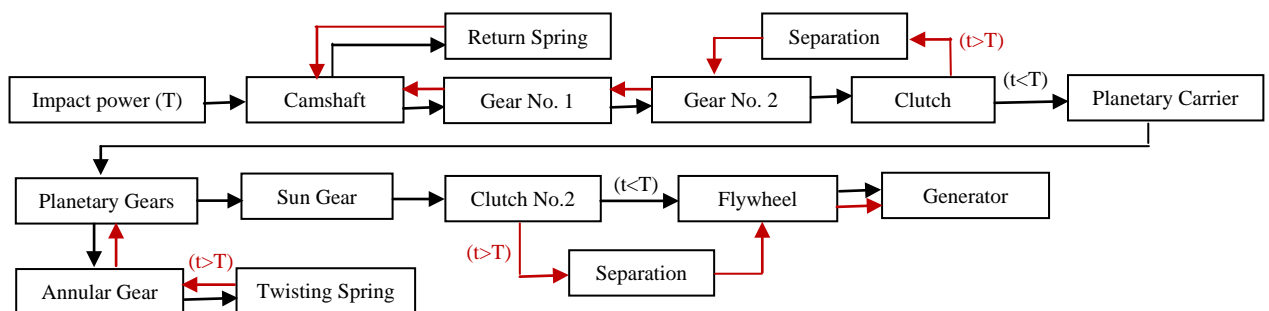
In the suggestion design generator core and flywheel system have coupled directly to rotate in the same angular speed, therefore equation (7) can be express according to flywheel angular speed as the following:

$$P_o = D_{em} \Omega_f^2 \tag{8}$$

Maximizing of harvested power in form of electricity is leading to maximization of flywheel angular speed and electromagnetic damping D_{em} .

4. OVERALL SYSTEM MODELING :-

Suggestion Design has many motions as plotted below in flowchart and the system motions are.



4.1. Motion Modeling During Load Effect (t<T).

Any simple epicyclic gear train should have six arrangement types of input output and fixed gear. But the best mechanism is choosing in this paper depending on the design simulation results comparison; however, this paper will modeling only the mechanism showing in **Fig. 7**, as a case study. Then, according to the global coordinate, the equivalent inertias are defined as the following:

$$I_{11} = I_s + I_f + 2I_s N_{s1}^2 + (I_c + I_{G2})N_{c1}^2 + (I_{G1} + I_{c\alpha})N_{c1}^2 \left(\frac{r_{G2}}{r_{G1}}\right)^2 \quad (9)$$

$$I_{22} = I_\alpha + 2I_s N_{s2}^2 + (I_c + I_{G2})N_{c2}^2 + (I_{G1} + I_{c\alpha})N_{c2}^2 \left(\frac{r_{G2}}{r_{G1}}\right)^2 \quad (10)$$

$$I_{12} = 2I_s N_{s1} N_{s2} + (I_c + I_{G2})N_{c1} N_{c2} + (I_{G1} + I_{c\alpha})N_{c1} N_{c2} \left(\frac{r_{G2}}{r_{G1}}\right)^2 \quad (11)$$

The equivalent stiffness constants are defined as:

$$K_{11} = k_1 N_{c1}^2 \left(\frac{r_{G2}}{r_{G1}}\right)^2 \quad (12)$$

$$K_{22} = k_2 + k_1 N_{c2}^2 \left(\frac{r_{G2}}{r_{G1}}\right)^2 \quad (13)$$

$$K_{12} = k_1 N_{c1} N_{c2} \left(\frac{r_{G2}}{r_{G1}}\right)^2 \quad (14)$$

The equivalent damping coefficients are defined as:

$$C_{11} = D_{em} + F_s + 2F_s N_{s1}^2 + F_c N_{c1}^2 + F_{c\alpha} N_{c1}^2 \left(\frac{r_{G2}}{r_{G1}}\right)^2 \quad (15)$$

$$C_{22} = F_\alpha + 2F_s N_{s2}^2 + F_c N_{c2}^2 + F_{c\alpha} N_{c2}^2 \left(\frac{r_{G2}}{r_{G1}}\right)^2 \quad (16)$$

$$C_{12} = 2F_s N_{s1} N_{s2} + F_c N_{c1} N_{c2} + F_{c\alpha} N_{c1} N_{c2} \left(\frac{r_{G2}}{r_{G1}}\right)^2 \quad (17)$$

and the equivalent components of the input torque are defined as:

$$T_{u1}(t) = T_u * N_{c1} * \left(\frac{r_{G2}}{r_{G1}}\right)^2 \quad (18)$$

$$T_{u2}(t) = T_u * N_{c2} * \left(\frac{r_{G2}}{r_{G1}}\right)^2 \quad (19)$$

by sum equations (9,10,11,12,13,14,15,16,17,18 and 19) and rearranged in a Lagrange matrix according to the definition of angular displacement, velocity and acceleration of the coordinates (β_1, β_2) , then, system definition of equation of motion can be extracted as the following:

$$\begin{bmatrix} I_{11} & I_{12} \\ I_{12} & I_{22} \end{bmatrix} \begin{bmatrix} \ddot{\beta}_1 \\ \ddot{\beta}_2 \end{bmatrix} + \begin{bmatrix} C_{11} & C_{12} \\ C_{12} & C_{22} \end{bmatrix} \begin{bmatrix} \dot{\beta}_1 \\ \dot{\beta}_2 \end{bmatrix} + \begin{bmatrix} K_{11} & K_{12} \\ K_{12} & K_{22} \end{bmatrix} \begin{bmatrix} \beta_1 \\ \beta_2 \end{bmatrix} = \begin{bmatrix} T_{u1}(t) \\ T_{u2}(t) \end{bmatrix} \quad (20)$$

Damping matrix in equation (20) has two different sources, friction damp source and electromagnetic damp source. Friction damp should be calculated by real prototype test, and cannot be calculated in the theoretical design, therefor we will assume a reasonable friction damping ratio ($\xi = 1$) and sum it with the calculated relatively large electromagnetic damp to estimate a realistic damping matrix.

Then by calculation of Eigen value, Eigen vector and making normalization for inertia, damping and stiffness matrices of equation (20), and rearranged the results in matrix form, we get:

$$\begin{bmatrix} I_1 & 0 \\ 0 & I_2 \end{bmatrix} \begin{bmatrix} \ddot{\beta}_{p1} \\ \ddot{\beta}_{p2} \end{bmatrix} + \begin{bmatrix} C_1 & 0 \\ 0 & C_2 \end{bmatrix} \begin{bmatrix} \dot{\beta}_{p1} \\ \dot{\beta}_{p2} \end{bmatrix} + \begin{bmatrix} K_1 & 0 \\ 0 & K_2 \end{bmatrix} \begin{bmatrix} \beta_{p1} \\ \beta_{p2} \end{bmatrix} = \begin{bmatrix} T_{p1} \\ T_{p2} \end{bmatrix} \quad (21)$$

System coordinates in equation (21) have transferred into principal. Equation (21) can be expressed as following form:

$$\ddot{\beta}_{p1} + 2\xi_1\omega_1\dot{\beta}_{p1} + \omega_1^2 \beta_{p1} = \left(\frac{1}{I_1}\right) T_{p1} \quad (22)$$

$$\ddot{\beta}_{p2} + 2\xi_2\omega_2\dot{\beta}_{p2} + \omega_2^2 \beta_{p2} = \left(\frac{1}{I_2}\right) T_{p2} \quad (23)$$

In the suggestion design input load has very short time interval, then, to solve equations (22) and (23) should be defined by "Duhamel Integral" with principal coordinates as the following:

$$\begin{aligned} \therefore \beta_{p1,2} = & \frac{\dot{\beta}_{p1,2}(0)}{\omega_{d1,2}} \sin(\omega_{1,2}t) + \beta_{p1,2}(0) \cos(\omega_{1,2}t) + \frac{1}{I_{1,2} \omega_{d1,2}} * \\ & * \int_0^t T_{p1,2} \cdot \exp(-\xi_{1,2} \omega_{1,2}(t - \tau)) \sin \omega_{d1,2}(t - \tau) d\tau \end{aligned} \quad (24)$$

Where $(\dot{\beta}_{p1,2}(0) \text{ and } \beta_{p1,2}(0))$ are an initial velocity and displacement of principal coordinates respectively, (τ) numerical step of time interval, and (ω_d) system natural frequency with damping system. Equation (24) can be expressed in the numerical form as the following: (Clough 1975)

$$\begin{aligned} \beta_{p1,2} = & \frac{\dot{\beta}_{p1,2}(0)}{\omega_{1,2}} \sin(\omega_{1,2}t) + \beta_{p1,2}(0) \cos(\omega_{1,2}t) \\ & + A(t) \sin \omega_{d1,2}t - B(t) \cos \omega_{d1,2}t \end{aligned} \quad (25)$$

Where

$$A(t) = \frac{\exp(-\xi \omega_{1,2}t)}{\omega_{d1,2}} \int_{t_1}^{t_2} T_{p1,2}(\tau) \exp(\xi \omega_{1,2}\tau) \cos \omega_{d1,2}\tau d\tau$$

$$B(t) = \frac{\exp(-\xi \omega_{1,2}t)}{\omega_{d1,2}} \int_{t_1}^{t_2} T_{p1,2}(\tau) \exp(\xi \omega_{1,2}\tau) \sin \omega_{d1,2}\tau d\tau$$

By using trapezium rule, $A(t)$ and $B(t)$ can be expressed in numerical form with equal steps of time interval ($\Delta\tau$), as the following: (Clough 1975)

$$\begin{aligned} A(t) &= A(t - \Delta\tau) + \frac{\Delta\tau}{2\omega_{d_{1,2}}} \exp(-\xi\omega_{1,2}t) \\ &\quad \times [T_{p_{1,2}}(t - \Delta\tau) \exp\{-\xi\omega_{1,2}(t - \Delta\tau)\} \cos \omega_{d_{1,2}}(t - \Delta\tau) \\ &\quad + T_{p_{1,2}}(t) \exp(-\xi\omega_{1,2}t) \cos \omega_{d_{1,2}}t] \\ &= A(t - \Delta\tau) + \\ &\quad \frac{\Delta\tau}{2\omega_d} [T_{p_{1,2}}(t - \Delta\tau) \exp(-\xi\omega_{1,2}\Delta\tau) \cos \omega_{d_{1,2}}(t - \Delta\tau) + T_{p_{1,2}} \cos \omega_{d_{1,2}}t] \end{aligned}$$

B (t) is calculated using a similar expression with the cosine functions replaced by sine functions. The accuracy of solution given by this procedure will depend upon the choice of $\Delta\tau$. It should be chosen small enough to ensure the loading history and the trigonometric functions are accurately defined.

4.2. System Modeling After Load Stroke End ($t > T$).

At the moment of the end of the load stroke, flywheel- generator system should be separated by the clutch system from epicyclic gear system. At this time, output power will be driven by storage flywheel kinetic energy. Electromagnetic generator has relatively large damping and tried to absorb flywheel energy. Flywheel-generator equation of motion can be express in Lagrange definition, as a single degree of freedom with damping system and no load effect. In big generator, inside magnetic field will effect as stiffness while for small generator, magnetic field is small too and stiffness energy can be neglected (Norton 2004). Then, after separation, equation of motion of flywheel-generator system can be defined as the following:

$$I_f \frac{d^2\theta_f}{dt^2} + D_{em} \frac{d\theta_f}{dt} + k\theta_f = 0 \quad (26)$$

$$\text{where } k = 0, \quad \frac{d\theta_f}{dt} = \Omega_f, \quad \text{and} \quad \frac{d^2\theta_f}{dt^2} = \frac{d\Omega_f}{dt}$$

$$\therefore \frac{d\Omega_f}{dt} = - \left(\frac{D_{em}}{I_f} \right) \frac{d\theta_f}{dt} \quad (27)$$

Especial solution of Lagrange Equation has needed and found of initial angular flywheel distance and velocity to solve equation (27). Electromagnetic damping coefficient (D_{em}) was defined in equation (5). Then, after separation, flywheel initial conditions are defined as the result of equations (25) at ($t = T$) after transfer the coordinate in time domain. Then equation (27) initial displacement and velocity can be defined as:

$$\theta_f(0) = \theta_f(T) \quad \text{and} \quad \Omega_f(0) = \Omega_f(T)$$

Then, solution of equation (27) can be solved as the following (Rudra 2001):

$$\theta_f(t) = \theta_f(T) + \frac{I_f \cdot \Omega_f(T)}{D_{em}} (1 - e^{-D_{em} \cdot t / I_f}) \tag{28}$$

and gradient of angular speed of flywheel-generator system after separation is defined as:

$$\Omega_f(t) = \Omega_f(T) \cdot e^{-D_{em} \cdot t / I_f} \tag{29}$$

Then, overall flywheel angular speed can be defined as:

$$\therefore \Omega_f(t) = \begin{cases} \frac{d}{dt} (Equ. 25) & (before\ separation) & t < T \\ \Omega_f(T) \cdot e^{-D_{em} \cdot t / I_f} & (after\ separation) & t > T \end{cases}$$

5. DESIGN SIMULATION AND LIMITATION OF ELEMENTS DIMENSIONS :-

Fig. 8 shows a smoother curve of instant input torque with time according to the time history in **Table 1**, and definition of equation (1) at vehicle speed 20km/hr. **Fig. from 9 to 15** show results of application of equations (12, 13, and 27) in time domain, and display the effect of all design elements, as measures of radii of Gear No.1, Gear No.2, planetary gear, sun gear, annular gear, flywheel inertia and vehicles velocity. Main three motions are included in all mechanical test figures as, motion of camshaft angle, motion of twisting spring angle and flywheel angular velocity respectively. **Fig. 9** and **11** prove that radius of Gear No.1 and planetary gear should be as small as, while **Fig. 10** and **12** show that, radius of Gear No. 2 and sun gear should be large to reduce system inertia and effect of impact velocity. **Fig. 13** and **14** show the effect of camshaft return spring and twisting spring respectively, however, camshaft return spring should be as small as to reduce losses in impact energy, while twisting spring must be large enough to control annular gear. **Fig. 15** shows effect of inertia of flywheel. Inertia of flywheel should be equilibrium between mechanical response under load effect and driving of generator for long time after end of load stroke. However the best dimensions of design elements have displayed in **Table 2** as which concluded from simulation figures.

6. POWER SIMULATIONS AND REUSLTS DISCOSIONS :-

Fig. 16 shows overall system response for impact of single tire at vehicle speed (20km/hr). Output harvested power reaching to the maximum value after time (0.045sec) from start point. Tip of harvested power pulses have instant value exceeded of (5000watts) and mean harvested power is (1000watts). Power curve is sloping down directly after crossing the tip reaching to the zero after time (0.9 sec). Flywheel system charges with maximum kinetic energy at the end of the load stroke (t=T), while after separation when (t>T) harvested power curve dropping towards the zero according to type of absorption of flywheel kinetic energy. Vehicle dimensions and allowable minimum distances between any two followed vehicles should be assumed. According to definition of (A and B) in **Fig. 17**, in order to make simulation for strike of more than one vehicle, then distances of proposed (A and B) are A=7m and B= 2.5m. **Fig. 18** shows shape of overall harvested power when system strikes by two followed vehicles have dimensions according to the proposed dimensions. Mean harvested power is jumping to record (2000watts) in period time equals to (3sec). First flywheel-generator system be at rest, when system strikes by vehicle front wheel flywheel-generator system will be had small response because it started from the rest, while impact of the rear wheel benefit from new condition of residual kinetic energy storage in flywheel system;

therefore, system response will be large. If the distance (A) between any two followed cars is large, the system may be lost all the storage energy and fall down to the rest again before reaching the second car. **Fig. 19** and **20** produce effect of magnetic generator resist torque or the electromagnetic damping (D_{em}), when system impacts by six following vehicles have the same assumed dimensions (A and B). **Fig. 19** proves that for large ($D_{em}=0.4\text{N.m.s/rad}$), system able to harvest mean power (3692watts) but undesired harvested power curve because it has very sharp pulses with short time intervals. While the **Fig. 20** proves that for small (D_{em}) harvested mean power falls down to (1342watts), but it includes desired shape of harvested power and has normal pulses with continuous bases for all active time. That's mean for small ($D_{em}=0.05\text{N.m.s/rad}$), generator has small resisting torque and flywheel able to drive the generator for long time without stop until the next vehicle impact is reaching. **Fig. 21** shows the simulations of instant harvested power for (75) followed cars have random dimensions as ($A = 5$ to 15m and $B = 2$ to 2.8m), and random speed range (20 - 50km/hr), with average vehicles weight (1000kg).

7. CONCLUSIONS AND RECOMMENDATIONS :-

This paper suggested a new mechanical imagination design able to harvest energy from vehicles impact power, in addition to control speed of traveling vehicles in public roads.

Heads of the camshaft corners should be fitted smoothly to avoid the potential side effects on the driving experience.

Typically speed bumps are found to limit vehicle speed in public roads that's assisting to increase efficiency and performance of the suggestion mechanical design.

Idea of absorbing of impact power by using annular gear twisting spring design is most suitable methods to accelerate the flywheel smoothly from the rest and harvest energy on wide range of vehicle speed.

Flywheel-Generator system wins acceleration, directly from impact energy and indirectly from annular gear twisting spring return energy.

Application of Lagrange equation of motion and definition of Duhamel's equation with realistic boundary conditions gets more reasonable results and simulation curves.

Electromagnetic damping coefficient (D_{em}) should be small enough to improve type of harvested power and allow flywheel-generator system rotation for extra time.

Simulation results prove that (1000 Watts) of mean potential power is available per active cell, that's mean power bump design able to harvest (2000 watts) from each passing vehicle have average weight (1000kg) and speed range (10 - 30 km/h)

We are recommended to constructing a prototype and applied method of the suggested design to make comparison and publishing a further paper.

8. ACKNOWLEDGEMENTS :-

The authors wish to thank the assistance from mechanical department and college of engineering of Babylon University.

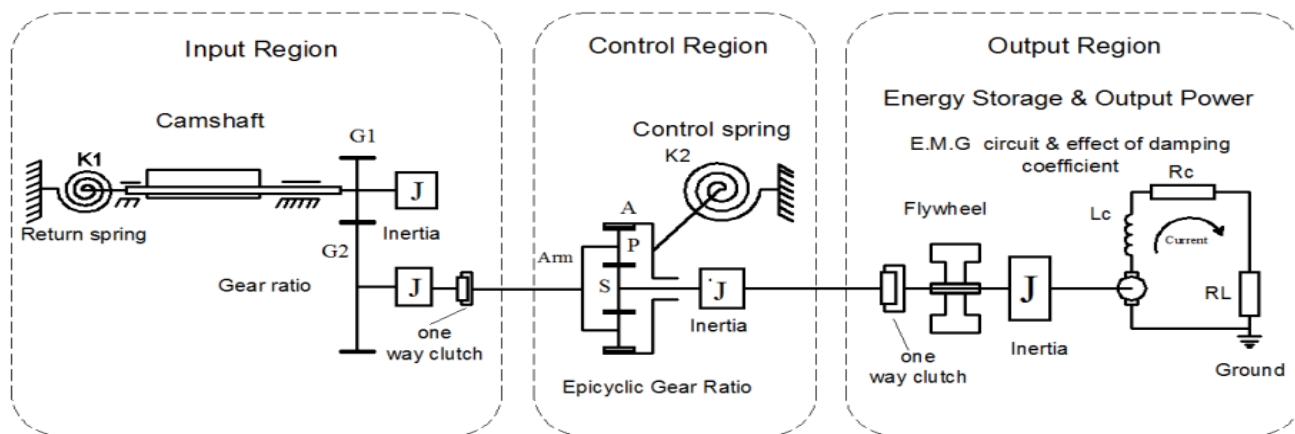


Fig. 3: Free body diagram of the suggestion mechanical speed bump design.

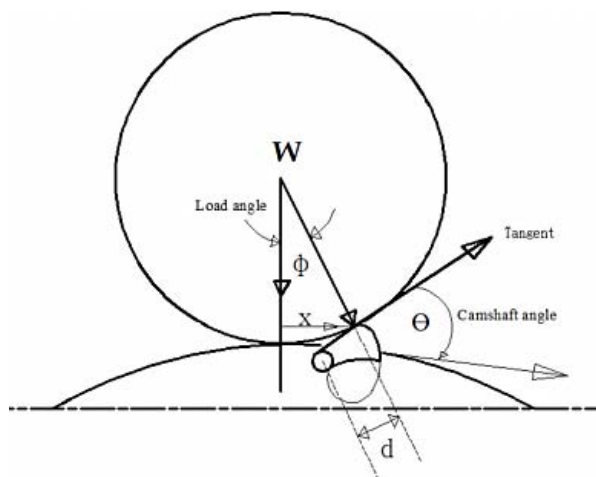


Fig. 4: Analysis of input load.

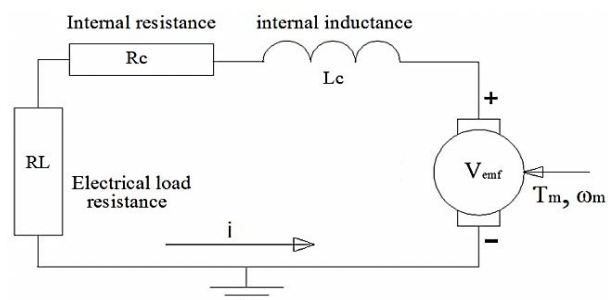


Fig. 6: Analysis of equivalent circuit of standard electromagnetic generator.

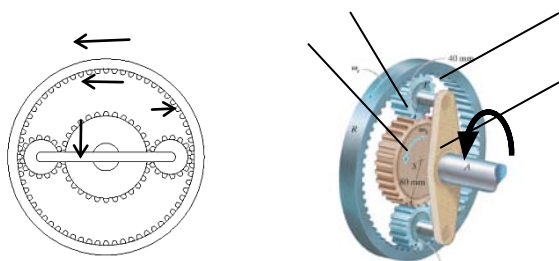


Fig. 5: Arrangement of epicyclic gear train.

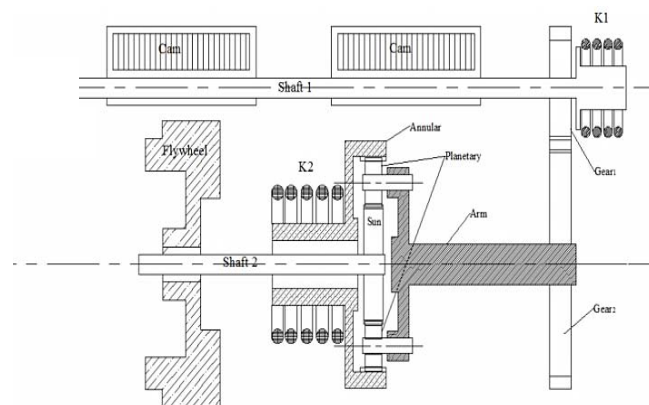


Fig. 7: Mechanism of suggestion mechanical speed bump design

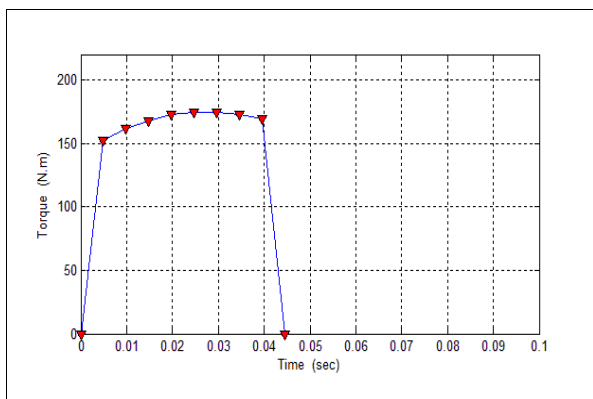


Fig. 8: Input torque simulation curve, at vehicle speed (20km/hr)

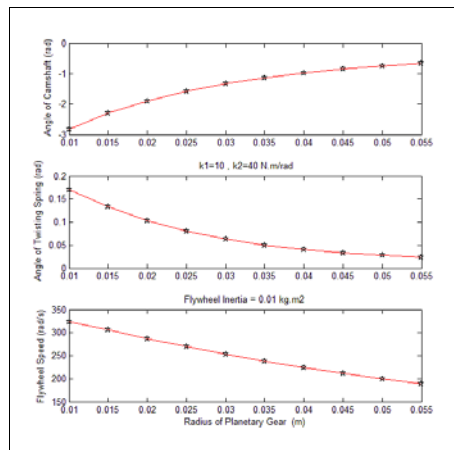


Fig. 11: Test of dimension of planetary gear.

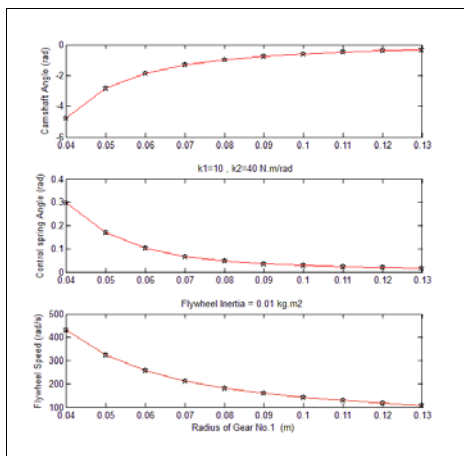


Fig. 9: Test of dimension of Gear No.1

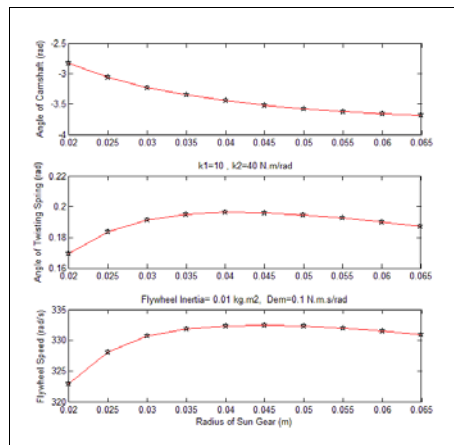


Fig. 12: Test of dimension of sun gear.

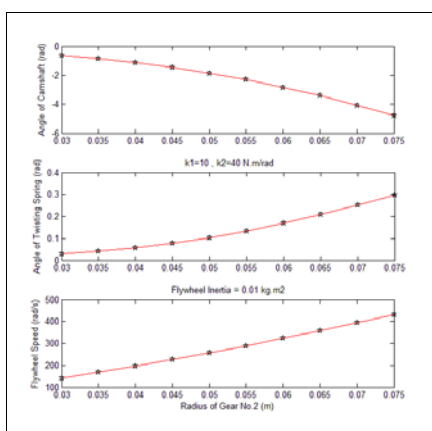


Fig. 10: Test of dimension Gear No.2

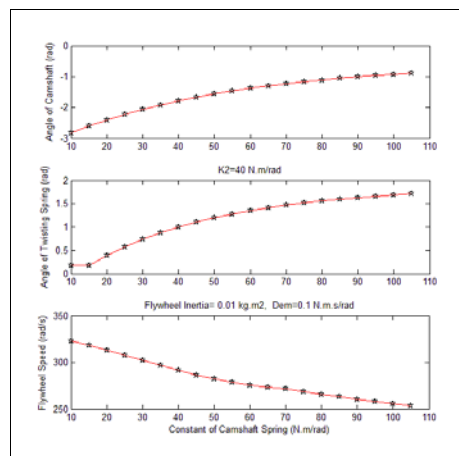


Fig. 13: Test of measuring of constant of camshaft return spring.

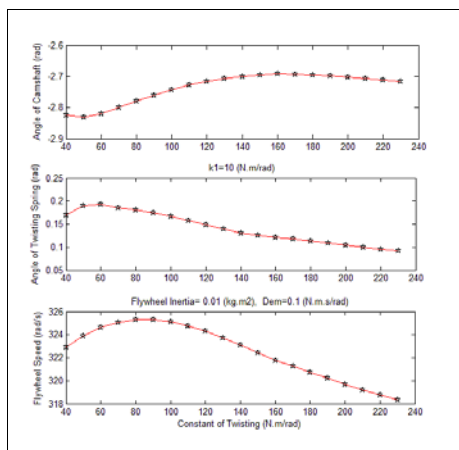


Fig. 14: Test of measuring of constant of twisting spring.

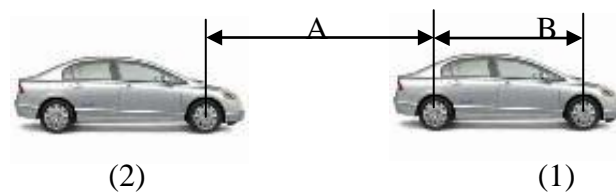


Fig. 17: Proposed defamation of any followed vehicle.

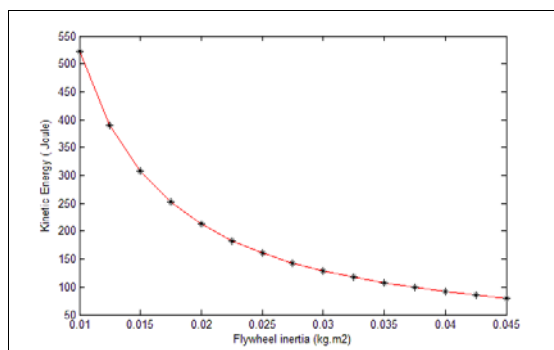


Fig. 15: Simulation of Flywheel Kinetic energy, for single impact with vehicle speed (20km/hr)

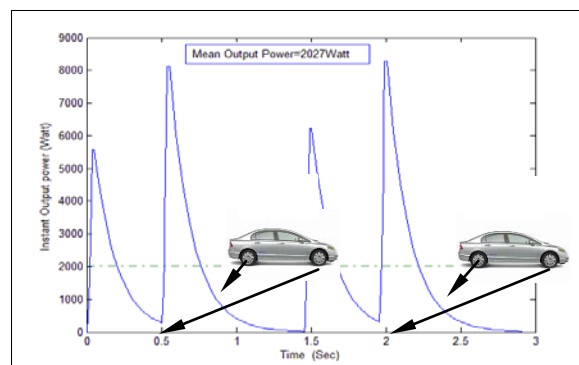


Fig. 18: Harvested power curve with time making by impacts of two vehicles.

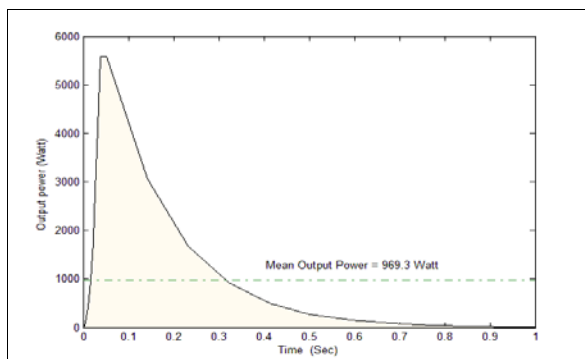


Fig. 16: Harvested power curve with time, for single impact with speed (20km/hr).

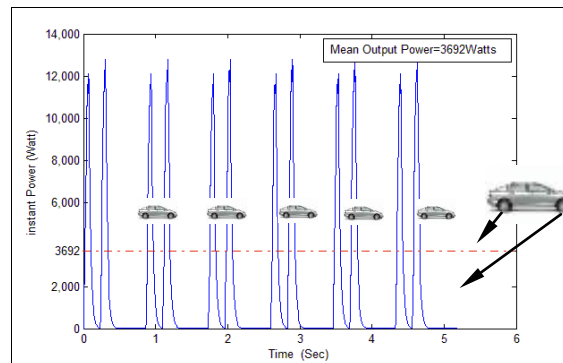


Fig. 19: Shape of harvested power by six vehicles (12 tire), with time, for large damping coefficient ($D_{em}=0.4N.m.s/rad$).

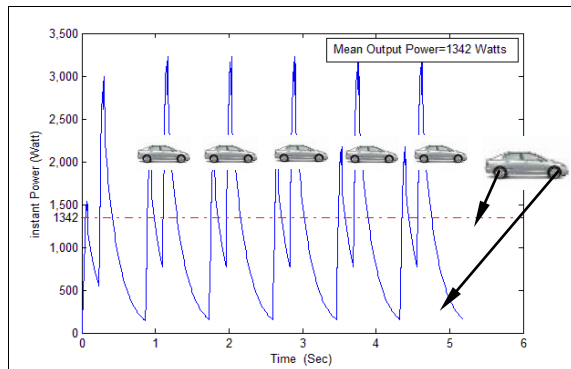


Fig. 20: Shape of harvested power by six vehicles (12 tire), with time, for small damping coefficient ($D_{em}=0.05N.m.s/rad$).

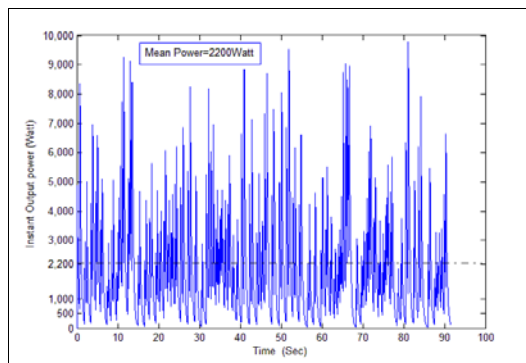


Fig. 21: Instant Harvested power with time, for (75) different vehicle type, at random speed (10-50km/hr) and random dimensions (A and B).

Table 1: Calculating of Time history and input torque, carried by 3Dmax program simulation.

Time (sec)	X (cm)	θ °(cam) (degree)	θ °(Load) (degree)	Distance (d) (cm)	Torque (N.m)
t ₀	0	45	15.7	6.47	0
t ₁	3	37	11.9	6.6	152.1
t ₂	6	30	8.3	6.9	161.18
t ₃	9	23	4.3	7	167.88
t ₄	12	17	0.2	7.1	172.34
t ₅	15	11	-4	7.15	174.58
t ₆	18	6	-8.4	7.1	174.70
t ₇	21	4	-12.8	7.29	172.78
t ₈	24	0	-17.6	7.2	168.88

Table 2: Best kinematic values of each moving elements concluded by design theoretical simulations, and mass properties are calculated by solid work program.

Substance	measure
Camshaft Inertia	0.008555 kg.m ²
Radius of Gear No.1	0.04m
Inertia of Gear No.1	0.001463 kg.m ²
Radius of Gear No.2	0.07m
Inertia of Gear No.2	0.00304 kg.m ²
Inertia of Annular Gear	0.001253kg.m ²
Radius of Sun Gear	0.02m
Inertia of Sun Gear	0.0001 kg.m ²
Radius of Planetary Gear	0.01m
Inertia of Planetary Gear	0.000002 kg.m ²
Inertia of planetary Carrier	0.000164 kg.m ²
Flywheel Inertia	0.015 kg.m ²
Constant of Twisting Spring	40 N.m/rad
Constant of Camshaft return Spring	10 N.m/rad
Assuming of friction damping ratio is (ζ)	0.1 without
Generator Damping (Dem)	0.1N.m.s/rad

REFERENCES

Avadhany, S., Abel, P., Tarasov, V. and Anderson, Z., 2009, "Regenerative Shock Absorber," U.S. Patent 0260935.

Ebrahimi, B., Khamesee, M., and Golnaraghi, M., 2008, "Feasibility Study of an Electromagnetic Shock Absorber with Position Sensing Capability," Proc. 34th Annual Conference of IEEE Industrial Electronics IECON, Vol. 1, pp. 2988–2991.

Goldner, R. B., Zerigian, P. and Hull, J. R., 2001, "A Preliminary Study of Energy Recovery in Vehicles by Using Regenerative Magnetic Shock Absorbers," SAE paper, Washington, D.C.

J.L.Meriam and L.G.Kraige "Engineering Mechanic Dynamics" volume 2 (1987)

Karnopp, D., 1989, "Permanent Magnet Linear Motors Used as Variable Mechanical Dampers for Vehicle Suspensions," *Vehicle System Dynamics*, Vol. 18, pp. 187- 200.

Martins, I., 2006, "Permanent-Magnets Linear Actuators Applicability in Automobile Active Suspensions", *IEEE Transactions on Vehicular Technology*, Vol. 55, pp. 86 94.

Norton, Robert L., ed. *Design of Machinery*. 3rd Ed. New York: McGraw- Hill, 2004.

Priya, S. & Inman, D. 2009. *Energy Harvesting Technologies*. Springer Science and Business Media.

Rudra Pratap and Andy Ruina, " *STATICS AND DYNAMICS*", Book, (2001) pp. 243-244.

R. W. Clough and J. Penzien, *Dynamics of Structures*. New York: McGraw-Hill (1975).

Suda, Y., Nakadai, S. and Nakano, K., 1998, "Hybrid Suspension System with Skyhook Control and Energy backlash friction backlash 8 Copyright © 2011 by ASME Regeneration", *Vehicle System Dynamics Supplement*, Vol. 28, pp. 619-634.

Zhang, Y., Yu, F. and Huang, K., 2009, "A State of the Art Review on Regenerative Vehicle Active Suspension," *International Conference on Mechanical Engineering and Mechanics*, Beijing, pp. 1689-1695.

Zuo, L., Scully, B., Shestani, J. and Zhou, Y., 2010, "Design and Characterization of an Electromagnetic Energy Harvester for Vehicle Suspensions," *Smart Material and Structures*, Vol. 19, pp. 1007-1016.